

**Seed-assisted hydrothermal synthesis of Sn-Beta for conversion of glucose to
methyl lactate: Effects of H₂O amount in the gel and crystallization time**

Xiaomei Yang^a, Liuyong Wang^a, Tianliang Lu^b, Beibei Gao^a, Yunlai Su^a and Lipeng

Zhou^{a*}

^a *Green Catalysis Center and College of Chemistry, Zhengzhou University, 100 Kexue Road, Zhengzhou 450001, China*

^b *School of Chemical Engineering, Zhengzhou University, 100 Kexue Road, Zhengzhou 450001, China*

* Tel.: +86 371 67781780; E-mail: zhoulipeng@zzu.edu.cn

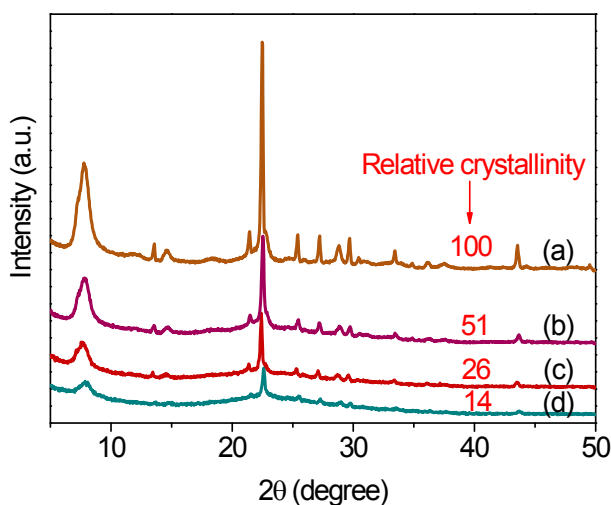


Fig. S1 XRD patterns of Sn-Beta crystallized at 140 °C for 3 d with $n_{\text{H}_2\text{O}}/n_{\text{SiO}_2}$ of (a) 4.5, (b) 5.5, (c) 6.5 and (d) 7.5.

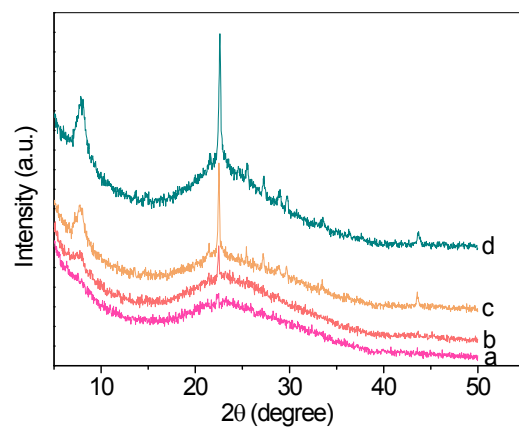


Fig. S2 XRD patterns of Sn-Beta-7.5 crystallized for different time. (a) 3 d without seed, (b) 7 d without seed, (c) 15 d without seed and (d) 3 d with seed.

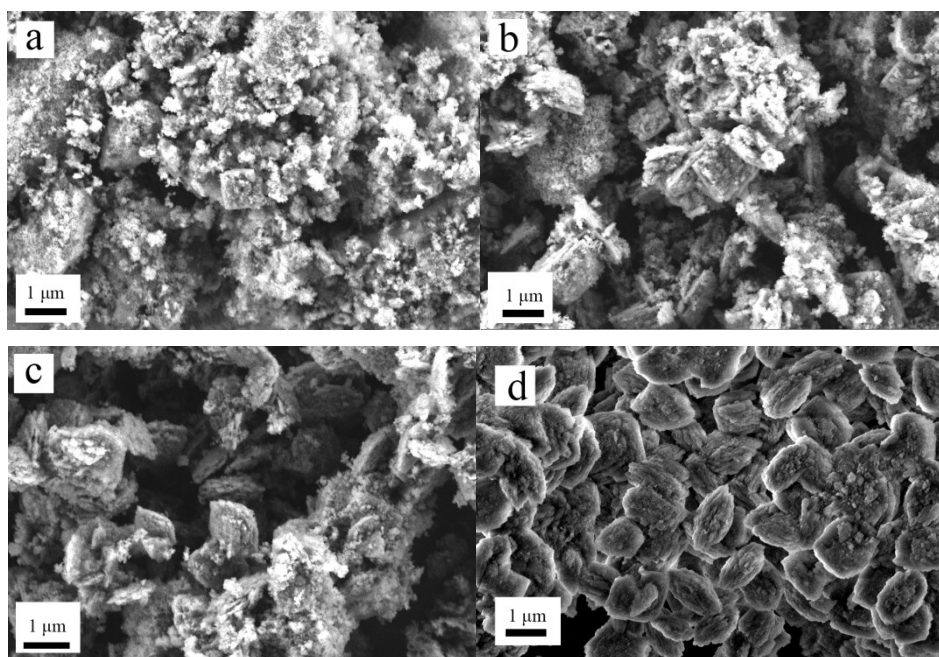


Fig. S3 SEM images of Sn-Beta crystallized at 140 °C for 3 days with $n_{\text{H}_2\text{O}}/n_{\text{SiO}_2}$ of (a) 7.5, (b) 6.5, (c) 5.5 and (d) 4.5.

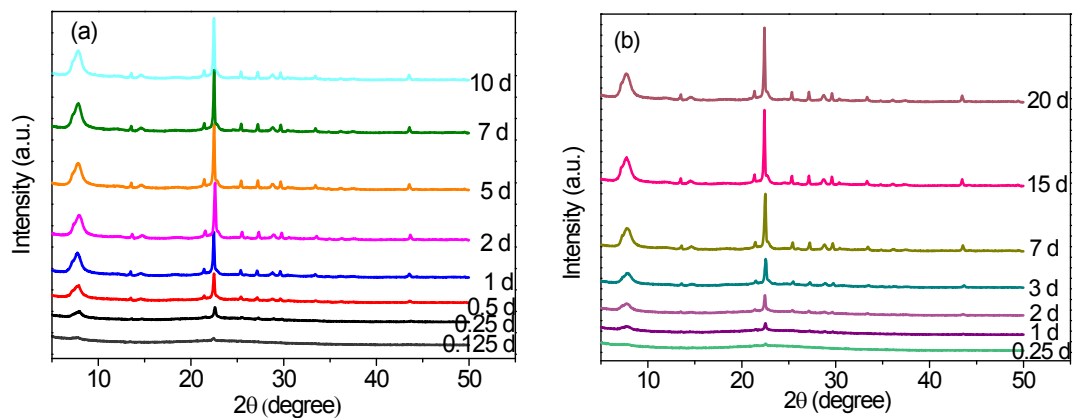


Fig. S4 XRD patterns of Sn-Beta at the $n_{\text{H}_2\text{O}}/n_{\text{SiO}_2}$ of (a) 4.5 and (b) 7.5.

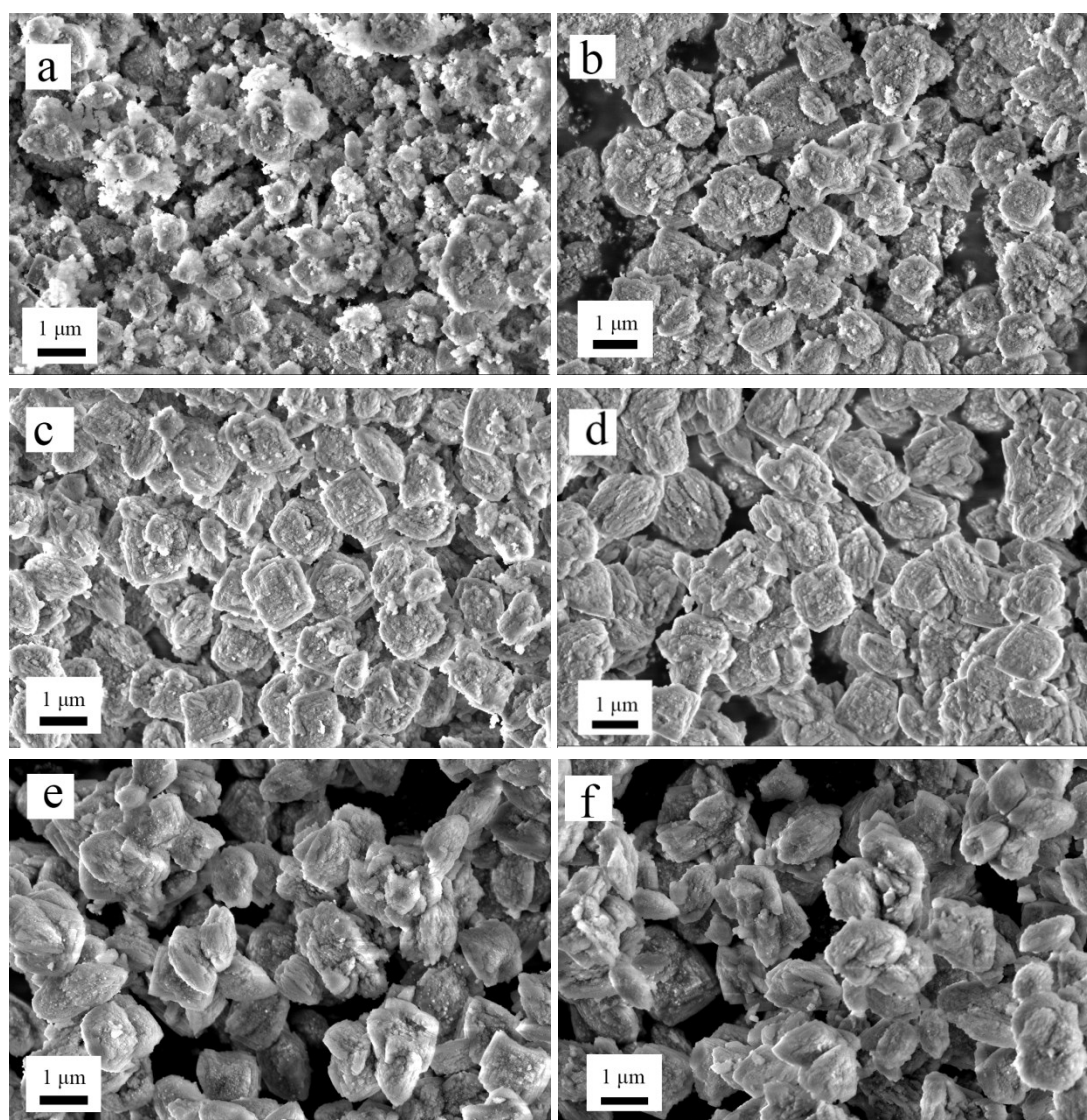


Fig. S5 SEM images of Sn-Beta obtained from the gel with $n_{\text{H}_2\text{O}}/n_{\text{SiO}_2}$ of 4.5. (a) 6 h, (b) 12 h, (c) 1 d, (d) 2 d, (e) 5 d, (f) 7 d.

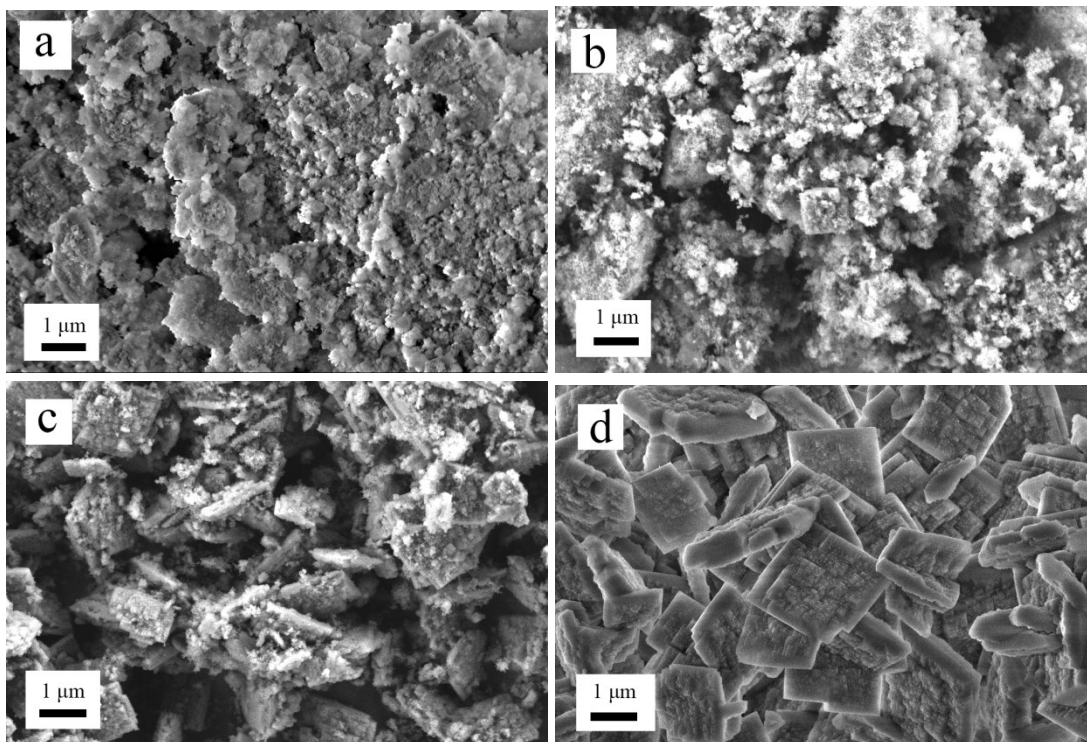


Fig. S6 SEM images of Sn-Beta obtained from the gel with $n_{\text{H}_2\text{O}}/n_{\text{SiO}_2}$ of 7.5. (a) 1 d, (b) 3 d, (c) 7 d, (d) 15 d.

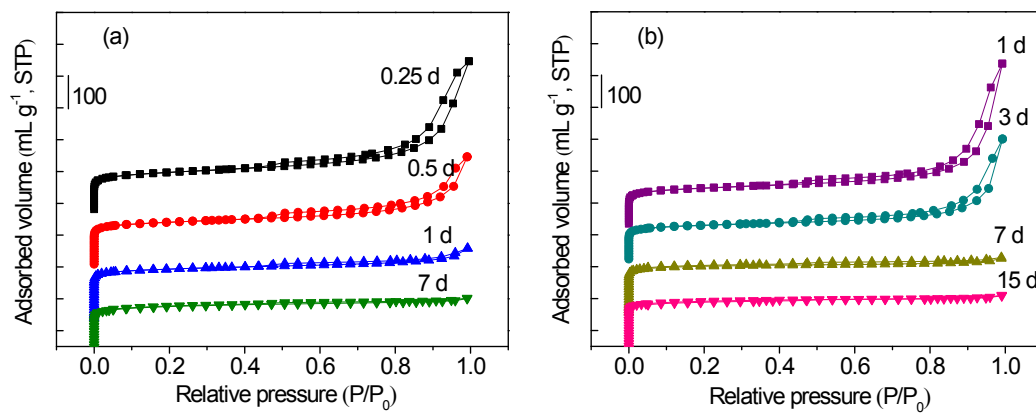


Fig. S7 N_2 isotherms of Sn-Beta-4.5 (a) and Sn-Beta-7.5 (b).

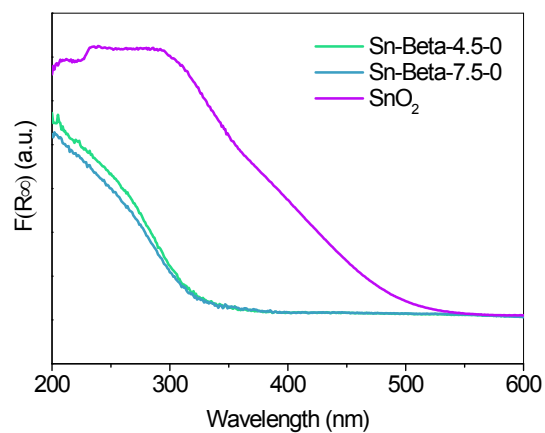


Fig. S8 UV-visible DR spectra of Sn-Beta-4.5 and Sn-Beta-7.5 without crystallization and bulk SnO₂.

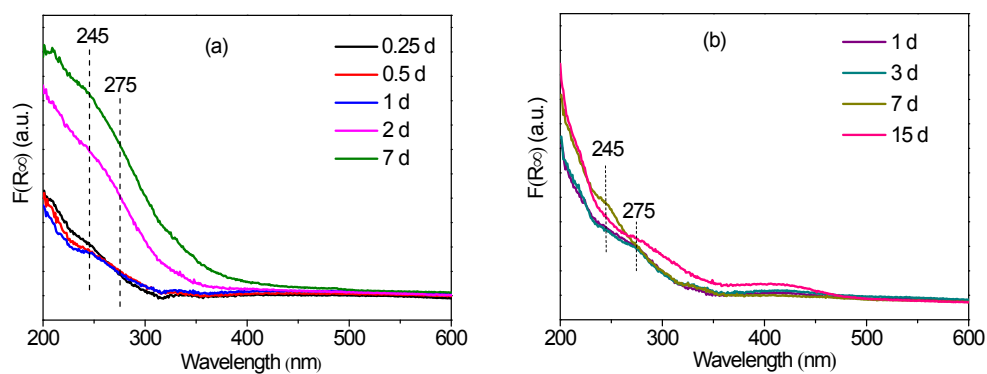


Fig. S9 UV-visible DR spectra of Sn-Beta-4.5 (a) and Sn-Beta-7.5 (b).

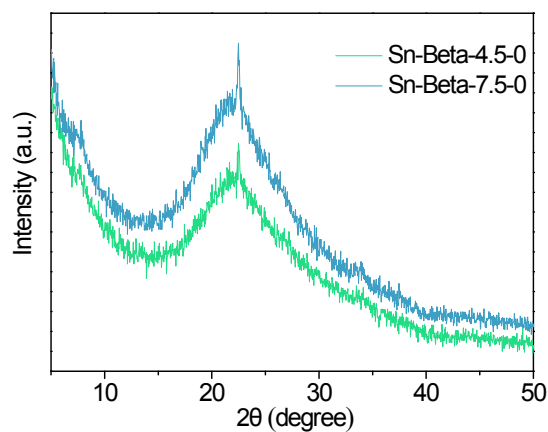


Fig. S10 XRD patterns of Sn-Beta without crystallization.

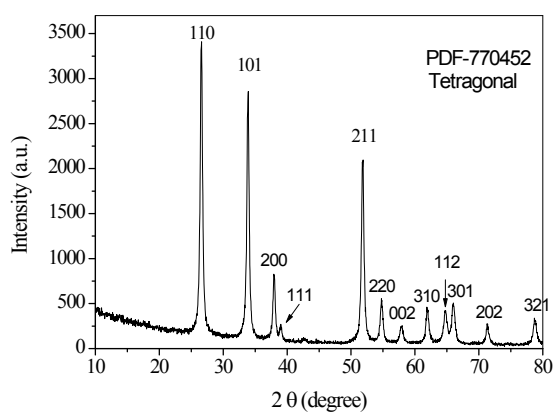


Fig. S11 XRD patterns of bulk SnO₂.

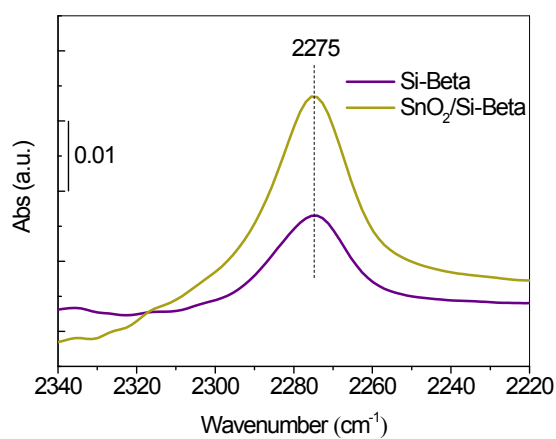
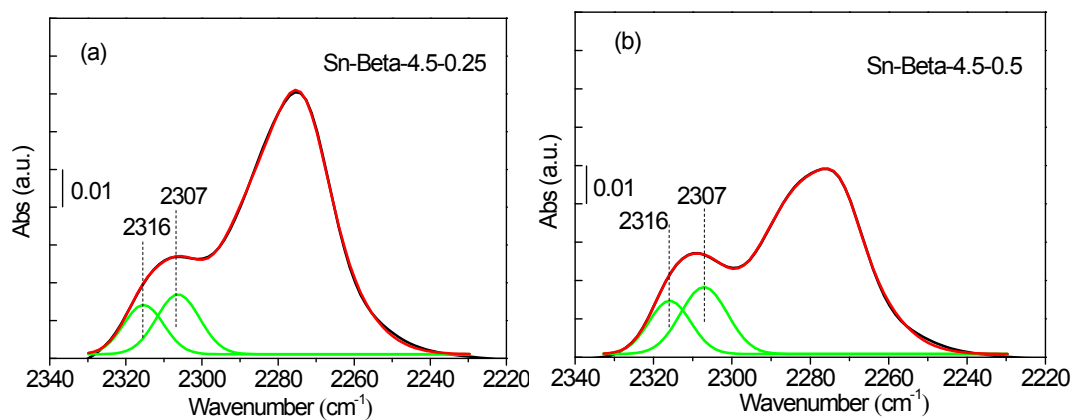


Fig. S12 FT-IR spectra of CD₃CN absorbed on Si-Beta and the mixture of SnO₂ and Si-Beta. The spectra were obtained after evacuation at room temperature for 15 min.



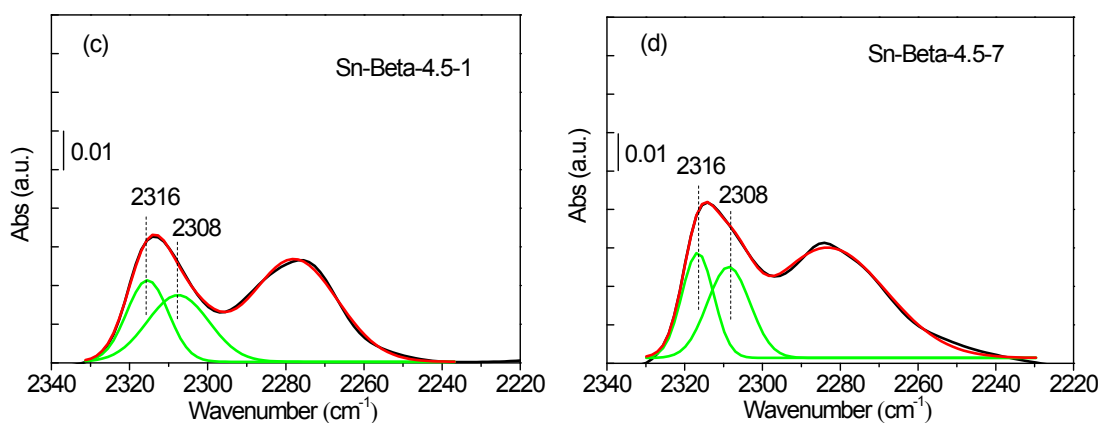


Fig. S13 Deconvolution of FT-IR spectra of CD₃CN adsorption on Sn-Beta-4.5. The spectra were obtained at room temperature after evacuation for 15 min.

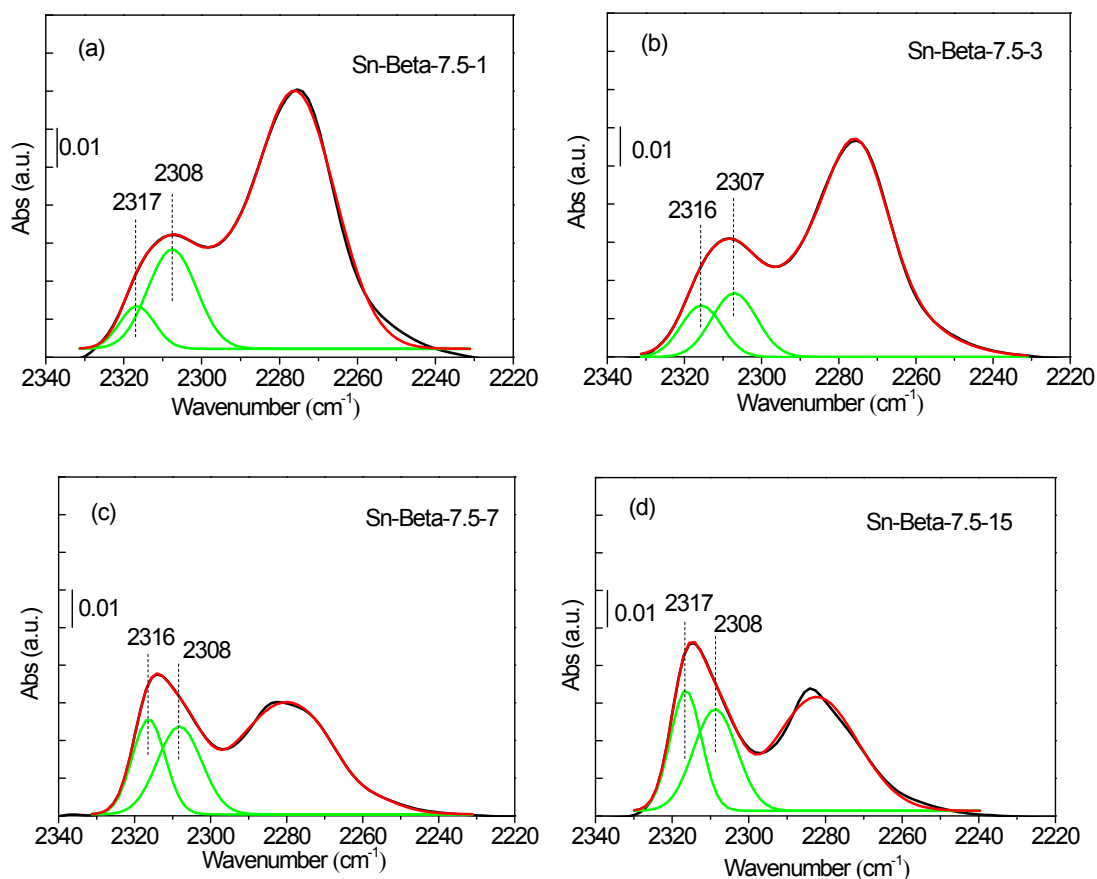


Fig. S14 Deconvolution of FT-IR spectra of CD₃CN adsorption on Sn-Beta-7.5. The spectra were obtained at room temperature after evacuation for 15 min.

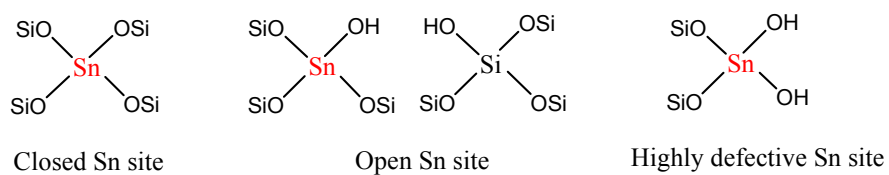


Fig. S15 Configurations of Lewis acid Sn site.

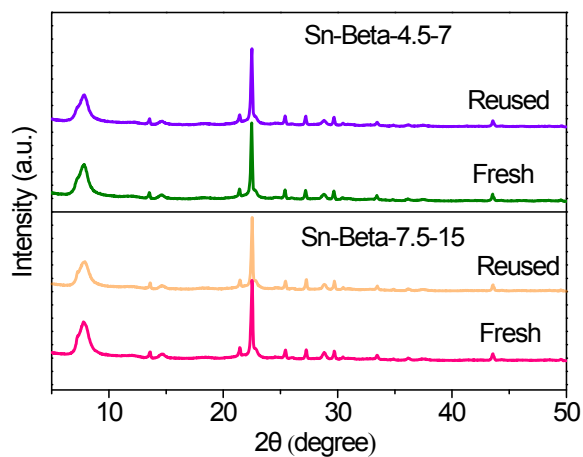


Fig. S16 XRD patterns of fresh and reused Sn-Beta-4.5-7 and Sn-Beta-7.5-15.

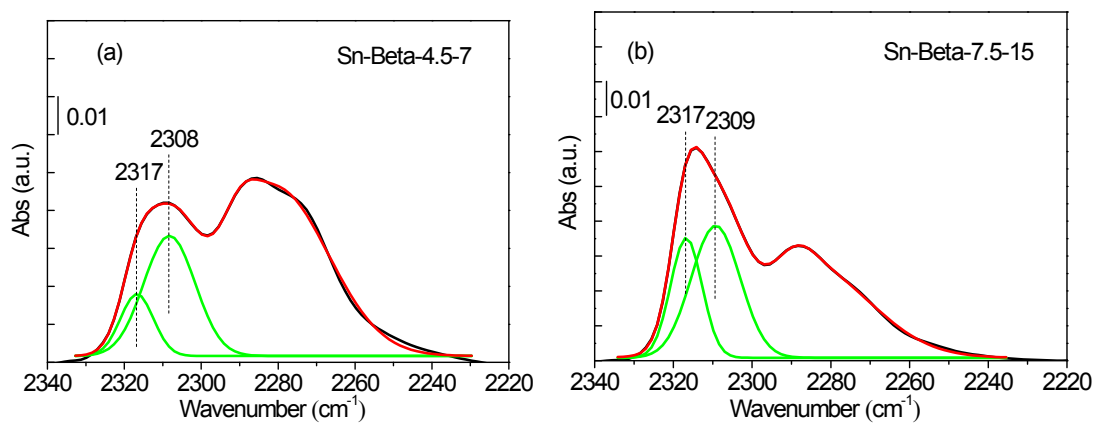


Fig. S17 Deconvolution of FT-IR spectra of CD₃CN adsorption on reused Sn-Beta.

The spectra were obtained after evacuation at room temperature for 15 min.

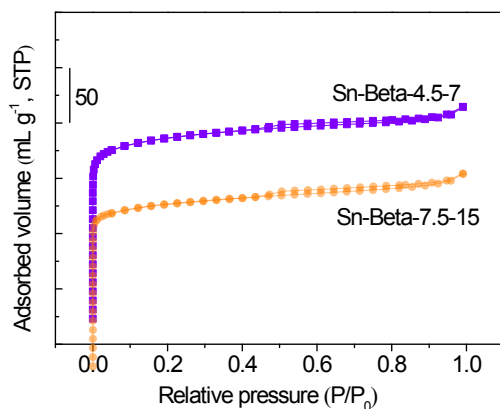


Fig. S18 N₂ isotherms of reused Sn-Beta-4.5-7 and Sn-Beta-7.5-15.

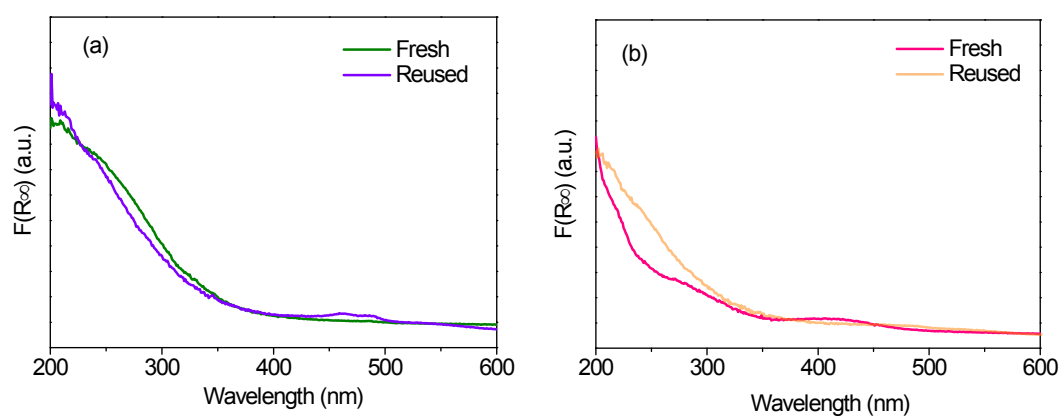


Fig. S19 UV-visible DR spectra of Sn-Beta-4.5-7 (a) and Sn-Beta-7.5-15 (b).

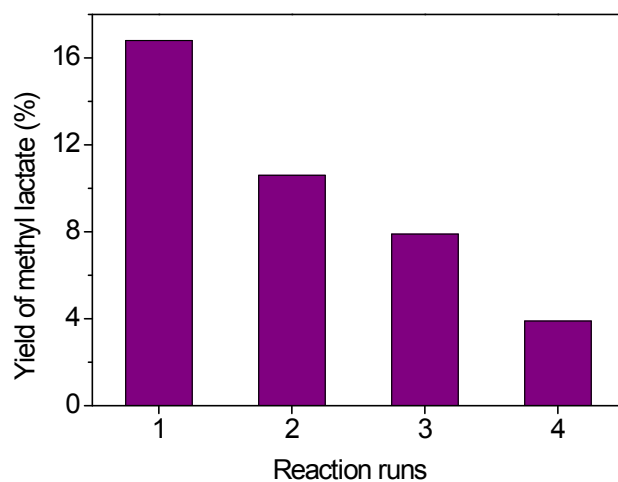


Fig. S20 Reusability of Sn-Beta-7.5-1 in the conversion of glucose to MLA.

Reaction conditions: glucose (0.20 g), catalyst (0.37 g), methanol (12 g), N₂ (0.4 MPa), 140 °C, 0.5 h.

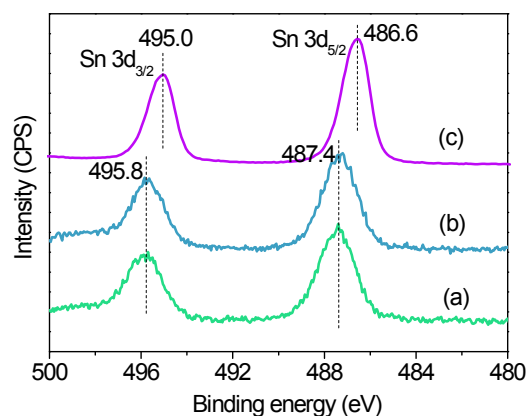


Fig. S21 XPS of Sn-Beta-4.5-0 (a), Sn-Beta-7.5-0 (b) and bulk SnO₂ (c).

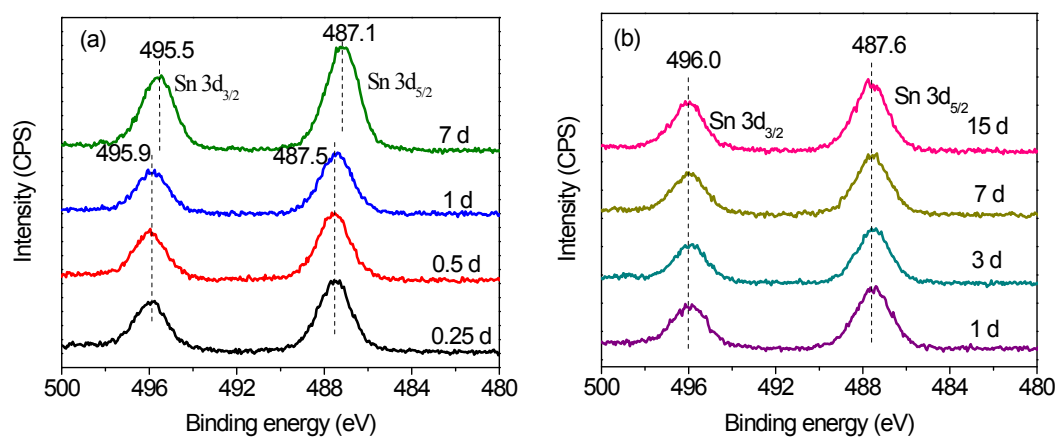


Fig. S22 XPS of Sn-Beta-4.5 (a) and Sn-Beta-7.5 (b).

XPS of bulk SnO₂ shows two signals at 495.0 eV and 486.6 eV (Fig. S21) corresponding to Sn 3d_{3/2} and Sn 3d_{5/2} photoelectrons of octahedrally-coordinated tin species. Though Sn species are also octahedrally-coordinated in Sn-Beta-4.5-0 and Sn-Beta-7.5-0, the signals shifted to higher binding energy (495.8 eV and 487.4 eV) due to that Sn species is highly dispersed. Except for Sn-Beta-4.5-7, Sn-Beta samples crystallized for different time give two signals at higher binding energy (496.0 eV and 487.6 eV) (Fig. S22) than highly dispersed octahedrally-coordinated Sn species, meaning that Sn species were in the tetrahedrally-coordinated framework sites. Of course, some Sn species at extraframework sites cannot be excluded. For Sn-Beta-4.5-7, the two signals shifted to lower binding energy (495.5 eV and 487.1 eV) than highly dispersed octahedrally-coordinated Sn species. It suggests that there

are more extraframework SnO₂ species in larger size, which agrees with the above results of SEM and UV-vis DRS.

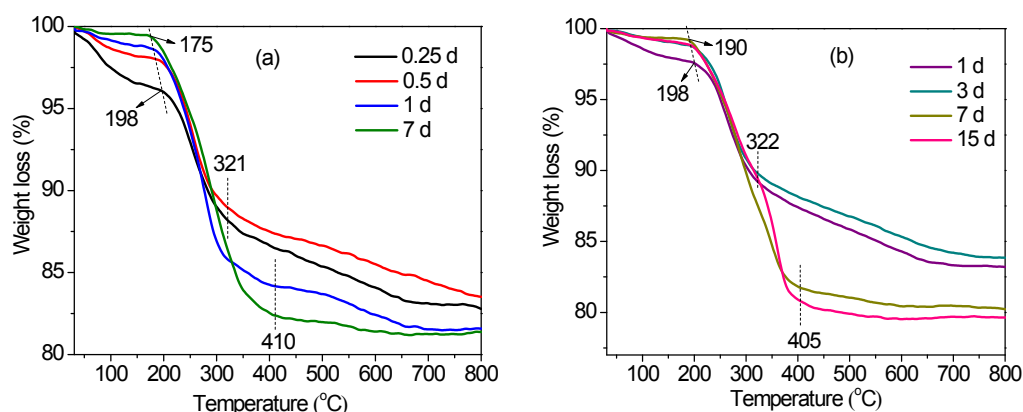


Fig. S23 TG analyses of Sn-Beta-4.5 (a) and Sn-Beta-7.5 (b).

Table S1 Percent weight loss of Sn-Beta-4.5 and Sn-Beta-7.5 from TG analyses

Sample	Weight loss (wt.%)		
	I	II	III
Sn-Beta-4.5-0.25	4.0	7.7	5.7
Sn-Beta-4.5-0.5	2.0	9.0	5.6
Sn-Beta-4.5-1	1.5	14.4	2.6
Sn-Beta-4.5-7	0.6	17.0	1.0
Sn-Beta-7.5-1	2.5	8.4	5.9
Sn-Beta-7.5-3	1.3	9.0	5.9
Sn-Beta-7.5-7	0.9	17.4	1.6
Sn-Beta-7.5-15	1.3	18.0	1.2

The TG curves of Sn-Beta-4.5 and Sn-Beta-7.5 presented in Fig. S23 can be divided into three stages. The first stage is at the temperature of < 200 °C, corresponding to the desorption of physisorbed water.¹ The second stage is attributed to the oxidation and decomposition of TEA⁺, which locates at temperature of < 410 °C.¹ The temperature of this stage for Sn-Beta samples with low crystallinity, such as Sn-Beta-4.5-0.25, Sn-Beta-4.5-0.5, Sn-Beta-7.5-1 and Sn-Beta-7.5-3, is lower than those with high crystallinity, which is at temperature of < 322 °C. The reason is

probably that the higher external surface and larger mesopore volume of the samples with low crystallinity facilitate the combustion of TEA⁺. The third stage can be ascribed to the desorption of water generated from silanol condensation. The weight loss of each stage is listed in Table S1. The weight loss of TEA⁺ increases with the crystallinity. It indicates more TEA⁺ species were occluded with the integration of zeolite framework structure. The weight loss of water in the samples with low crystallinity is much higher than the samples with high crystallinity, suggesting that the samples with low crystallinity have more silanols and are more hydrophilic.

Reference

1. Z. He, J. Wu, B. Gao and H. He, *ACS Appl. Mater. Interfaces*, 2015, **7**, 2424–2432.